nature ecology & evolution

ARTICLES

https://doi.org/10.1038/s41559-019-0879-1

Non-parametric estimation of the structural stability of non-equilibrium community dynamics

Simone Cenci* and Serguei Saavedra

Environmental factors are important drivers of community dynamics. Yet, despite extensive research, it is still extremely challenging to predict the effect of environmental changes on the dynamics of ecological communities. Equilibrium- and model-based approaches have provided a theoretical framework with which to investigate this problem systematically. However, the applicability of this framework to empirical data has been limited because equilibrium dynamics of populations within communities are seldom observed in nature and exact equations for community dynamics are rarely known. To overcome these limitations, here we develop a data-driven non-parametric framework to estimate the tolerance of non-equilibrium community dynamics to environmental perturbations (that is, their structural stability). Following our approach, we show that in non-equilibrium systems, structural stability can vary significantly across time. As a case study, we investigate the structural stability of a rocky intertidal community with dynamics at the edge of chaos. The structural stability of the community as a whole exhibited a clear seasonal pattern, despite the persistent chaotic dynamics of individual populations. Importantly, we show that this seasonal pattern of structural stability is causally driven by sea temperature. Overall, our approach provides novel opportunities for estimating the tolerance of ecological communities to environmental changes within a non-parametric framework.

Changes in environmental conditions affect biological populations through perturbations of ecological parameters[1,2]. For example, it is well known that fluctuations of temperature, salinity and pH significantly affect the growth rate of bacteria in marine communities[3]. Similarly, it has been shown that climate change has strong impacts on species interactions[4,5]. However, predicting the effects that the variability of environment-dependent parameters (for example, species interactions and growth rates) have on the dynamics of ecological communities has proved to be far more challenging due to the ubiquitous nonlinearities and state-dependent behaviour of natural ecosystems[6]. Yet, this knowledge is key for understanding and anticipating the responses of ecological communities to environmental changes[7].

Numerous studies have shown that a theoretical framework to estimate the effect of parameter perturbations on nonlinear dynamics can be built based on the concept of structural stability[8–15] (that is, the stability of the qualitative behaviour of a dynamical system against perturbations of its parameters). These approaches either assume a specific parametric model for the dynamics[12] or are non-parametric but assume the convergence to locally or globally stable equilibrium points[13]. Therefore, the applicability of these approaches for the analysis of empirical data has been limited by the fact that the true governing equations of community dynamics are rarely known[16–18], and equilibrium dynamics are rarely observed in natural ecosystems[6,19–21].

To overcome these limitations, here, we develop a data-driven non-parametric approach to study the structural stability of non-equilibrium dynamical systems (Box 1). As a prototype for nonlinear dynamics, we consider chaotic systems. This choice is motivated by the growing evidence that ecological communities can exhibit chaotic dynamics not only in closed controlled experiments but also in the field[19,22–25]. However, our approach is valid for any type of nonlinear dynamics. Then, using synthetic data, we show that structural stability in chaotic systems can vary significantly across time. That is, the tolerance of ecological communities to equivalent perturbations can change depending on the timing of their occurrence. Finally, using empirical data from a rocky intertidal community that exhibits dynamics at the edge of chaos[25], we show that the structural stability of this community follows a clear seasonal pattern mediated by changing environmental conditions.

Before presenting our theoretical framework, it is important to stress that our study is not the first to propose a non-parametric approach to studying the stability of ecological communities[21]. Yet, in contrast with previous work, here, we focus on structural stability rather than dynamical stability. These are two complementary but very distinct concepts. Dynamical stability measures the response of a system to a perturbation or fluctuation in the state variables (that is, species abundances). Instead, structural stability measures the response of a system to perturbations in its parameters (for example, species interactions and growth rates) or the model itself. While the importance of structural stability in community dynamics is becoming increasingly clear[11–14], to the best of our knowledge, no previous study has attempted to measure this form of stability non-parametrically from empirical data without assumptions of equilibrium dynamics. In this context, our work attempts to close this gap and shed new light on the mechanisms driving the dynamics of ecological communities.

Results

Validation on synthetic data. To test the validity of our proposed measure of local structural stability (see Box 1), we analysed synthetic data from eight chaotic dynamical systems (details about the models can be found in Supplementary Section 1). Specifically, for each chaotic model, we ran the following analysis. First, we generated a random perturbation of the parameters. Then, we applied this same perturbation on two different points on the attractor and compared the effect of the perturbation on the trajectories with the VCR at the two points. Finally, we repeated this process 1,000 times for each chaotic model (see Methods for a more detailed description of the simulation).

Department of Civil and Environmental Engineering, Massachusetts Institute of Technology, Cambridge, MA, USA. *e-mail: cenci@mit.edu

Box 1 | Theoretical framework

To illustrate our approach, we considered chaotic time series generated by some unknown dynamical system:

$$\dot{\mathbf{x}} = \mathbf{f}(\mathbf{x}, \boldsymbol{\eta}) \quad (1)$$

where $\mathbf{f} \in C^1$ is a vector field (or model), $\mathbf{x} \in \mathbb{R}^d$ is the state vector (that is, species abundance), and $\boldsymbol{\eta}$ is a vector of environment-dependent parameters (for example, rates of interactions or growth rates). In an empirical setting, the solution of the unknown system in equation (1) provides the observational time series that can be collected from an experiment or field observations. Here, we assume that the time series has a deterministic component stronger than the noise level and that the trajectories lie on an attractor $\mathcal{M}$. Note that these are standard assumptions in nonlinear time-series analyses[33,35].

Time-dependent response to changing environments. To understand the derivation of our proposed measure, recall that, loosely speaking, a system is structurally stable if small changes to the parameters (or the model itself) do not induce large changes in the dynamics[36]. Note that, here, we consider the definition of structural stability mostly adopted in the ecological literature[12,37,38]. More formally, a dynamical system is structurally stable if the topology of the phase portrait is preserved under smooth changes of the vector field[37]. Under both definitions, structural stability is a global property of a model (or vector field). However, a striking feature of chaotic systems (and nonlinear systems in general) is that the same parameter perturbation can have a different impact on the dynamics depending on the time of its occurrence. This phenomenon follows directly from local properties of chaotic attractors[39] and has been observed in natural ecosystems[40]. For example, it is well known that the effect of temperature on sardine stocks depends on the state of the system[6]. Thus, there is a need to study and understand how the structural stability of nonlinear systems changes locally along the model's trajectories.

To illustrate the state-dependent response of nonlinear dynamics to parameter perturbations, Fig. 1 shows the effect of a small perturbation in a single parameter (the beneficial effect of a resource on its consumer) on a chaotic consumer–resource model[26] (see Supplementary Section 1). The perturbation is applied at different times (t_1, …, t_n) to an otherwise unperturbed system (see Methods). Figure 1a shows that the extent to which the perturbed and unperturbed trajectories diverge from each other depends on the time at which the perturbation occurs. Figure 1b,c shows visual examples of a small and large effect of the perturbation on the trajectories, respectively. This example illustrates that in systems away from equilibrium points, the level of structural stability (measured here as the effect of a perturbation on the model's future trajectory) changes depending on the state of the system. Clearly, in a real setting, testing the effects of all possible perturbations is not a possibility. Therefore, to study the local structural stability of a chaotic (non-equilibrium) system more systematically, we need to investigate the local properties of the vector field along the attractor (that is, the model's trajectories).

Local structural stability of non-equilibrium dynamics. We propose the use of the volume contraction rate (VCR) of a non-equilibrium dynamical system as a measure of the local structural stability. Specifically, we show that the VCR and local structural stability are negatively related. The VCR is the divergence of the vector field[37] or, equivalently, the trace of the Jacobian matrix of $\mathbf{f}$ (that is, $\nabla \cdot \mathbf{f}(\mathbf{x}, \boldsymbol{\eta}) = \mathrm{Tr}J$). Because the Jacobian matrix is a function of the state vector (that is, species abundances, $J : J(\mathbf{x})$), the VCR changes with the state of the system. At each point on the attractor $\mathcal{M}$, the VCR can be negative or positive, or more generally, can be larger or smaller than at other points on $\mathcal{M}$. For small perturbations in the parameters, models generated by perturbations acting on states with a small VCR will continue to have a small VCR. Hence, these perturbed models will stay closer to the original model than models generated by perturbations acting on states with a large VCR.

The concepts above are illustrated in Fig. 2. A small (large) deviation between perturbed and unperturbed trajectories after a perturbation of the parameters captures the idea that vector fields with a small (large) VCR are weakly (strongly) affected by a perturbation to the parameters. That is, the smaller the VCR, the larger the local structural stability. Note that, following this definition, the local structural stability of chaotic systems is measured in relative terms. That is, a state is more or less structurally stable with respect to another state of the same system. Importantly, this negative relationship between VCR and structural stability must hold true on average because there is always an uncertainty associated with the direction towards which the parameter perturbation pushes the model and its trajectories. Here, we have provided a heuristic argument in favour of the VCR as a probabilistic measure of local structural stability, but not rigorous proof. Therefore, in the Results, we provide an extensive numerical validation of our hypothesis.

Figure 3 shows that, on average, perturbations on the parameters acting on points with a small VCR tend to generate trajectories that remain closer to the unperturbed trajectories (that is, large local structural stability) than perturbations acting on points with large VCR, (that is, small local structural stability). The closeness between trajectories was measured as the root-mean-square distance (RMSD) between perturbed and unperturbed state vectors on the attractor after the perturbation. The results of this analysis provide support to the hypothesis that the VCR is negatively related to the local structural stability of the dynamics. Therefore, the VCR can be used as a reliable probabilistic indicator of how much a trajectory will be perturbed by a perturbation to the parameters.

Analysis on empirical data. As a case study, we investigated the temporal evolution of the local structural stability of a rocky intertidal community in New Zealand that exhibits dynamics at the edge of chaos[25]. Supplementary Fig. 5 shows the time series of this community, and a detailed discussion of this dataset can be found in Methods. To estimate non-parametrically the Jacobian coefficients from the observational time series, we used the S-map algorithm developed in previous studies[26,27] plus an elastic-net regularization function[28] (see Methods and Supplementary Section 2). Because observational noise in the time series is not strictly Gaussian, to account for uncertainty in model selection, we used a non-parametric model-averaging technique[29] (see Methods and Supplementary Sections 2 and 3). Then, using the inferred Jacobian coefficients, we computed the value of the VCR (that is, $\mathrm{Tr}(J)$) at each point in time. Note that by using the S-map algorithm, we can recover the trace of the Jacobian up to a constant. However, because we are interested in both the local minima and maxima of the trace, only the trend

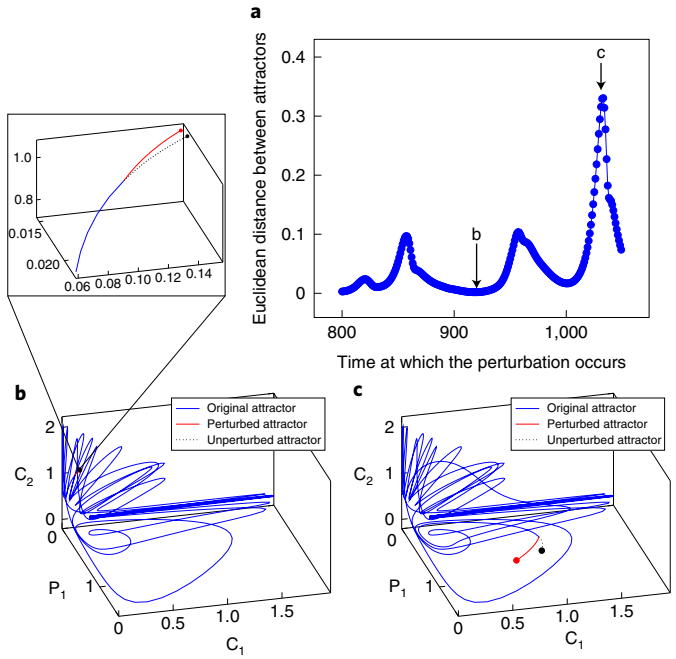

Fig. 1 | Parameter perturbations occurring at different points in time on a chaotic dynamical system can have different effects on its dynamics. a, Divergence of perturbed and unperturbed trajectories (measured by the Euclidean distance between attractors) when one parameter (ν_1 in Supplementary Equation (4)) of a consumer–resource chaotic model is changed at different points in time (that is, different points on the attractor). The *x* axis is the time at which the perturbation occurs. The *y* axis illustrates the effect of the perturbation. **b**,**c**, Effect of the perturbation at the least (**b**) and most (**c**) affected points. Three-dimensional projections of the five-dimensional original attractor (that is, the projection on the space of two consumers, C_1 and C_2, and one predator, P_1) are shown. The two circles illustrate the state of the system at time $t=3$ after the perturbation (that is, 300 points separated by a spacing $dt=0.01$). The distance between the two states (perturbed, red circle; unperturbed, black circle) is much larger in **c** than in **b**, even though the perturbation to the parameters was exactly the same. This figure illustrates how in nonlinear systems, perturbations acting at different points in time can have different impacts on the dynamics.

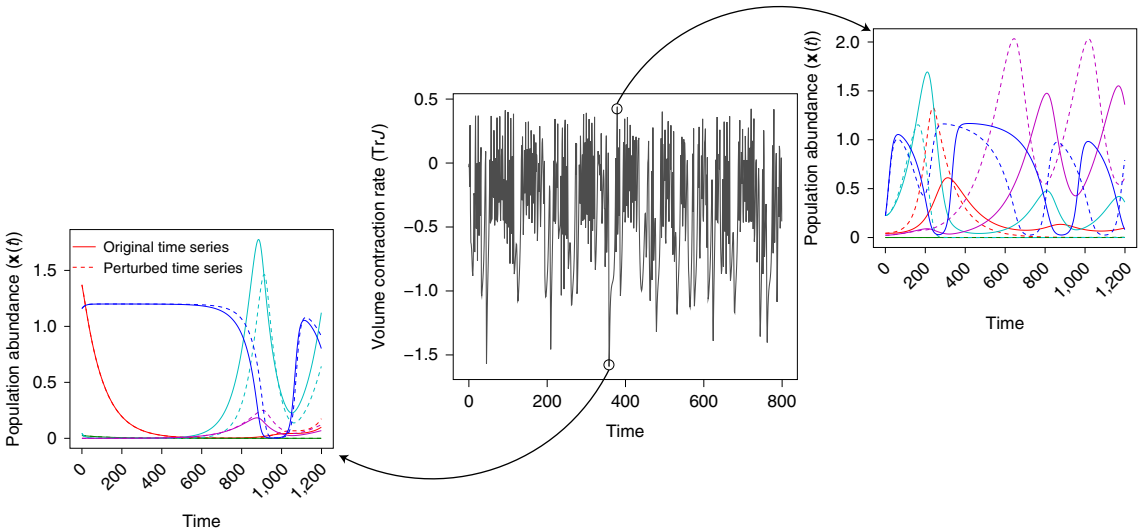

Fig. 2 | Perturbations acting on the parameters of a nonlinear system with large and small VCRs induce different effects on the trajectories. Middle, temporal changes of the VCR (that is, Tr*J*) for the same model as in Fig. 1. The left and right panels show the perturbed (dashed lines) and unperturbed (solid lines) trajectories (of all five species) in the most and least structurally stable states, respectively. This figure illustrates that the larger the VCR, the smaller the local structural stability of the system.

(and not the sign of the trace) should be considered as meaningful (Supplementary Fig. 3 shows the performance of the regularized S-map in inferring the trend of the VCR from time-series data under different distributions of noise).

Figure 4a shows that the local structural stability of the community fluctuates without showing any particular trend across the observation period. Importantly, these observed changes of structural stability have no clear associations with environmental

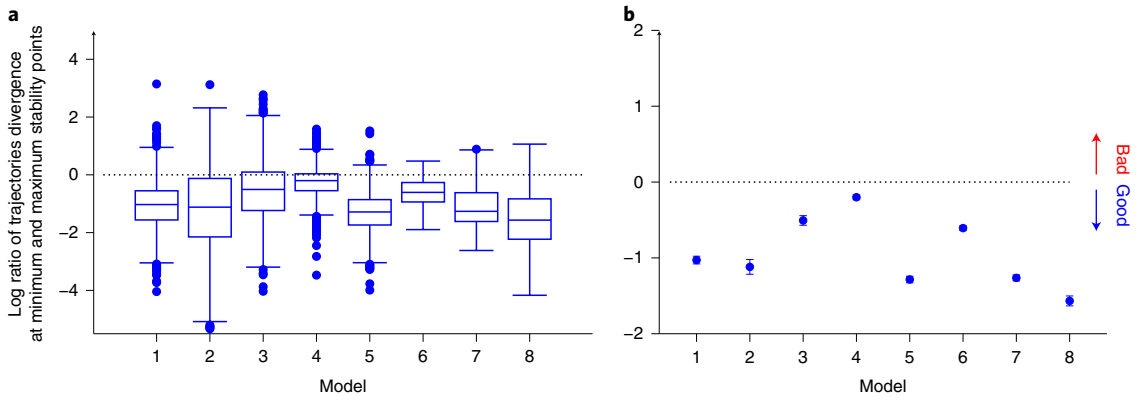

Fig. 3 | Validation on synthetic data. Logarithm of the ratio of the divergence of trajectories when the parameters are perturbed in the least and most structurally stable states (that is, $\log\left[\frac{d(x,\tilde{x})_{\text{maximum structural stability}}}{d(x,\tilde{x})_{\text{minimum structural stability}}}\right]$) over eight different chaotic models. **a**, Distribution over 1,000 realizations. **b**, Medians ± 95% confidence intervals, computed using a two-sided Wilcoxon test. Note that a median ratio of less than zero indicates that the VCR is a good measure of local structural stability. That is, the larger the VCR, the smaller the local structural stability of the system. See Supplementary Section 1 for a detailed description of the chaotic models.

parameters (Fig. 4b,c). This result is not surprising as environmental variables were not included in the reconstruction of the Jacobian matrix (which is a proxy only for biotic interactions) nor in the computation of the structural stability (which is only a function of the Jacobian coefficients). Yet, looking at the monthly average of structural stability throughout the years, Fig. 4d shows a clear seasonal pattern. That is, the community exhibits its minimum structural stability (that is, maximum VCR) in the summer and winter seasons, particularly in the warmest and coldest months (February and August, respectively; see Fig. 4e). In addition, we found that fluctuations of structural stability are strongly anticorrelated with the seasonal changes of mean wave height (Fig. 4f), which are known to play a significant role in the dynamics of rocky intertidal communities[30,31]. Overall, these findings suggest that environmental forcing can have an important effect on biotic interactions and, consequently, on the structural stability of this community.

To support our argument above, we need to distinguish between causal associations and spurious correlations formed between environmental variables and structural stability. For this purpose, we used convergent cross-mapping (CCM)[6]—a nonlinear causality test that is used to infer causal relationships among variables in nonlinear dynamical systems (see Methods for further details). Figure 5 (as well as Supplementary Figs. 8 and 9) shows the results of this analysis. First, we found that there is a strong causal relationship between species abundances. This confirms that species interactions are important drivers of the dynamics of this system (Supplementary Fig. 8). Second, we found a weakly statistically significant causal effect of sea temperature on the individual species abundances (apart from the abundance of algae; Supplementary Fig. 9). Instead, we found that sea temperature has a significant causal effect on the local structural stability of the system (Fig. 5a). That is, we found that sea temperature drives the dynamics of a collective property of the community. Note that previous work[25] has included temperature as a covariate in the analysis, and has shown that it is a driver of the dynamics. Here, we found the same results without explicitly adding this constraint (that is, temperature is not included in the estimation of the Jacobian coefficients). Finally, we found no causal relationship between mean wave height and local structural stability (Fig. 5b). Hence, this implies that the correlations observed in Fig. 4d,f are spurious.

Discussion

The increasing volume of available data in natural sciences is providing the scientific community with a unique opportunity to gain new insights into the complex dynamics of ecological communities. Non-parametric approaches provide a framework with which to leverage these new opportunities by overcoming the inherent limitations of generalizability on empirical datasets of equilibrium or model-based approaches[17,21]. In this context, the main motivation of our study has been to derive a generalizable, data-driven, non-parametric methodology to monitor the tolerance of ecological communities to environmental changes.

We have demonstrated the generalizability of our proposed methodology by showing that it can be successfully applied on several synthetic time-series data (Fig. 2). We then illustrated our approach on a long-term ecological study of a community that exhibits dynamics at the edge of chaos[25]. An important result derived from this analysis is that we have been able to give evidence to the hypothesis established in previous work[25]: that sea temperature is a causal driver of the dynamics of this community. Importantly, we have obtained these results without including temperature as a covariate in our analysis and without formulating any parametric model to explain the data.

On a more general and conceptual level, the most important insight of our results is that they provide evidence in support of the idea that it is possible to build ecological theories without the formulation of explicit parametric models. We believe that non-parametric theories are a particularly exciting and promising avenue of research in ecological studies. Other studies are already moving in this direction[6,17,18,21]. For example, previous work[21] has shown that it is possible to measure the dynamical stability of non-equilibrium communities within a non-parametric framework. Our work is complementary to these previous studies[21]. Indeed, as discussed in the introduction, structural stability and dynamical stability are two distinct but complementary concepts. This difference for the case study presented here is illustrated in Supplementary Fig. 7, which plots the yearly and monthly fluctuations of the real part of the largest eigenvalue of the Jacobian matrix (that is, dynamical stability), showing that the pattern of dynamical stability is significantly different from the pattern of local structural stability.

Another important application of our approach, which is outside the scope of this work but can be the subject of future research, is the possibility of using our derived measure of local structural stability to estimate the local predictability of nonlinear ecological time series in changing environments. In fact, following our approach, structurally unstable points are those that are strongly affected by environmental perturbations and, therefore, we expect them to

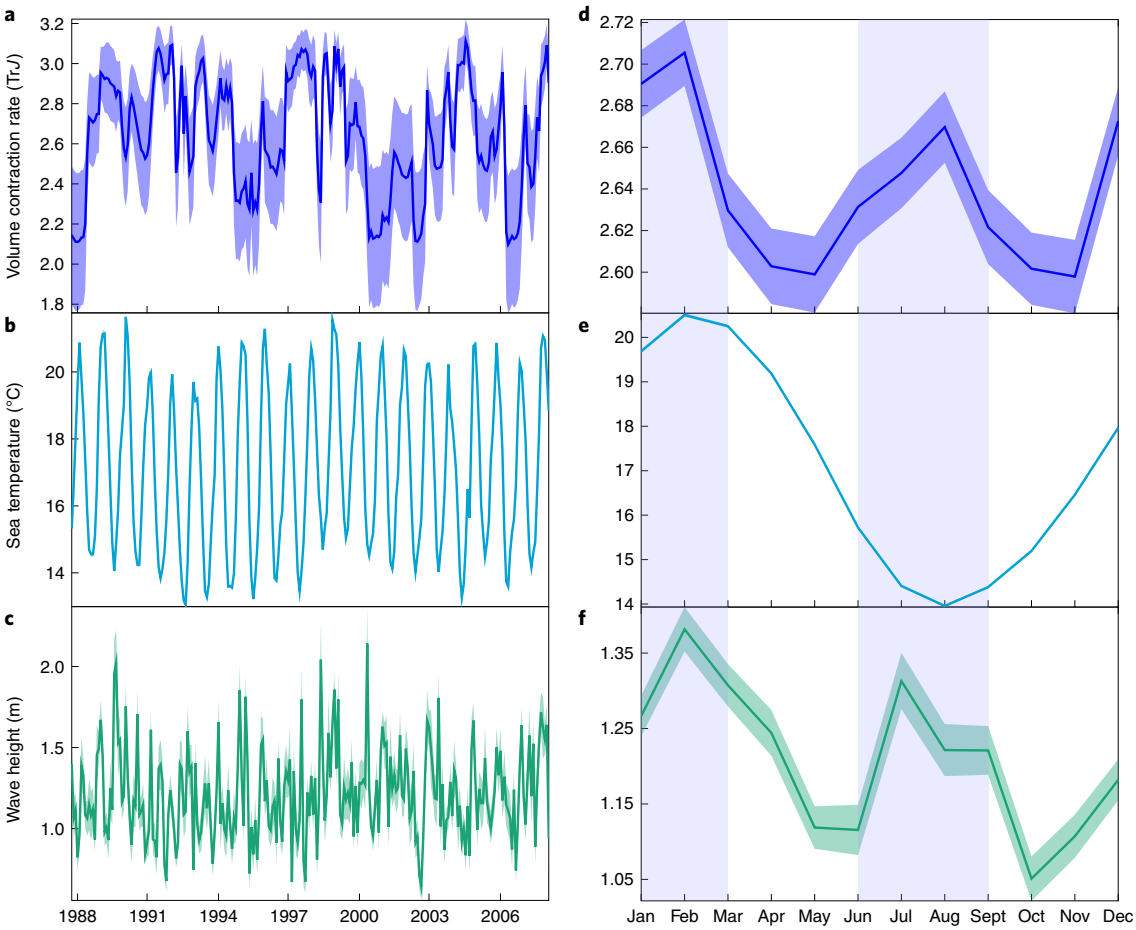

Fig. 4 | Structural stability pattern of a rocky intertidal community at the edge of chaos. a–**c**, Fluctuations of the trace of the Jacobian (that is, the VCR inferred from the S-map; **c**), sea temperature (**b**) and wave height (**c**). **d**–**f**, Monthly average of these respective quantities across the observation period. The blue bands in **d**–**f** represent winter and summer. Importantly, **d** shows that the structural stability of this community follows a clear seasonal pattern. That is, the maximum local structural stability (and therefore minimum VCR) is observed in the spring and autumn seasons when waves are smaller and sea temperatures are milder. The error bands in **a** and **d** were computed from the ensemble method described in the Supplementary Information. The error bands in **b**, **c**, **e** and **f** represent the s.e.m. of the aggregate data.

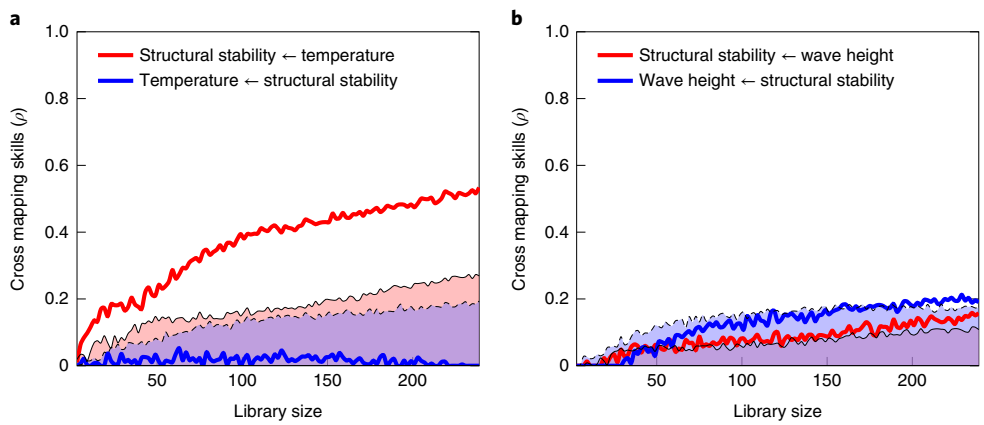

Fig. 5 | CCM test. Results of the causal analysis discussed in the Methods. Shaded areas correspond to 95th percentiles of the causality test run on the surrogate time series (providing a null expectation). A causal link is statistically significant if the CCM skills (correlation coefficients ρ) increase with the library size and are above the null expectations. **a**, Sea temperature is a causal driver of the local structural stability (that is, the VCR) of the rocky intertidal community. **b**, There is no statistically significant causal relationship between the local structural stability and mean wave height.

be the most difficult to predict when systems evolve in continuously changing environments. Hence, our approach could be used to associate an uncertainty level with ecological forecasts for community dynamics.

Overall, we have found that, despite relying on minimal assumptions, our approach provides results on empirical data that match with intuition. That is, the local structural stability of ecological communities changes as a function of environmental conditions. Given the generalizability of our approach to nonlinear systems, we foresee important applications on many different empirical studies. Specifically, we believe that this study can set out the foundations for data-driven, model-free research to monitor and anticipate the responses of ecological communities to the pressing increasing rates of environmental changes.

Methods

Time-dependent responses in nonlinear systems. To illustrate how the same perturbation can have different effects on the dynamics depending on the time of its occurrence (that is, Fig. 1), we ran the following analysis. (1) We fixed the perturbations to a chaotic dynamical system. Specifically, we perturbed the parameter ν_1 from $\nu_1 = 0.1$ to $\tilde{\nu}_1 = 0.15$ in model 3 in Supplementary Section 1. This is a five-species consumer–resource chaotic model. (2) We integrated the dynamics up to a time t_1. Following previous work[26], we chose initial conditions such that we ensured that $\mathbf{x}(t_1)$ was on the attractor. (3) We integrated the model with the perturbed parameters ($\tilde{\nu}_1$) and initial conditions $\mathbf{x}(t_1)$. After the perturbation, we ran the dynamics for 300 integration steps with spacing $dt = 0.01$. (4) Then, we measured the RMSD of the perturbed and unperturbed trajectories. (5) Finally, we repeated steps (2)–(4) n times to produce each point in Fig. 1a. The values on the x axis are the times $t_1, \ldots, t_n$. The values on the y axis are the Euclidean distances between perturbed and unperturbed trajectories. Overall, Fig. 1 shows the state-dependent effect of a parameter perturbation on nonlinear systems.

Numerical simulations for the validation on synthetic data. As discussed in the main text, to test systematically the validity of our proposed measure, we computed the relative RMSD of trajectories over an ensemble of parameter perturbations occurring at different times. Specifically, we integrated a chaotic dynamical system until the trajectories converged on the attractor $\mathcal{M}$. This convergence was ensured by integrating the differential equation for a long period of time before starting the simulation. Moreover, for many of the tested models, initial conditions that converged quickly to the attractor were taken from the literature. Then, we perturbed a random number of parameters with normally distributed noise with zero mean and standard deviation proportional to a random fraction of the perturbed parameter. For example, for a given parameter μ, we have $\mu_{\text{perturbed}} = \mu_{\text{unperturbed}} + \eta$, where $\eta \sim \mathcal{N}(0, \mu_{\text{unperturbed}}/\kappa)$ and $\kappa \sim \mathcal{U}(2, 10)$. The number of perturbed parameters was a random number drawn from a uniform distribution. Then, we randomly selected two points on the attractor by randomly sampling below (above) the 15th lower (upper) percentile of TrJ. This value was chosen by studying how the RMSD between perturbed and unperturbed trajectories varies as a function of the percentile, as shown in Supplementary Fig. 2. Then, we again integrated the model with the perturbed parameters and measured the RMSD between perturbed and unperturbed trajectories. Finally, we took the logarithm of the ratio between the RMSD of the trajectories perturbed at the point in time with maximum structural stability to the one with minimum structural stability. For our measure to be valid, this ratio needs to be less than zero (that is, perturbations to the parameters occurring in structurally stable states have weaker effects on trajectories than perturbations to the parameters occurring in states that are less structurally stable). Then, we repeated the same procedure 1,000 times over 8 distinct chaotic models. The results are shown in Fig. 3, which shows both the distribution over all of the realizations (Fig. 3a) and the median and 95% confidence intervals computed using a two-sided Wilcoxon signed rank test (Fig. 3b).

Inference of the Jacobian matrix. To infer the Jacobian matrix, we used the S-map[26,27] with an additional elastic-net regularization term[29]. That is, for each point on the attractor, we solved the following minimization problem:

$$\hat{c} = \underset{c \in \mathbb{R}^d}{\operatorname{argmin}} \frac{1}{n}(Y - Xc)^T K_\theta(X, X^\star)(Y - Xc) + \lambda((1-\alpha)\|c\|_1 + \alpha \|c\|_2^2) \qquad (2)$$

where $\mathbf{c}$ is a row of the Jacobian matrix, X is the data matrix and Y is the variable to predict. The parameters $\alpha \in (0, 1)$ and $\lambda \in \mathbb{R}_+$ are two regularization parameters selected with leave-one-out cross-validation. $K_\theta(X, X^\star)$ is a kernel function with bandwidth θ. Note that the S-map is a locally weighted regression model. The weights are kernel functions with diagonal elements $K_\theta(\mathbf{x}, \mathbf{x}^\star) = D\left(\frac{\|\mathbf{x} - \mathbf{x}^\star\|}{\theta}\right)$. In contrast with standard local regression schemes, the weighting in the S-map is based on distances between points on the attractor in the state space rather than their distance in time[26]. Notice that, because the S-map is a form of local regression, the number of points required for an accurate reconstruction of the parameters grows exponentially with the dimensionality of the system[32]. Here, we have 250 data points in a four-dimensional system; hence, the S-map is a perfect candidate for the inference of Jacobian coefficients. See Supplementary Sections 2 and 3 for more details on the inference method, together with a numerical example.

Empirical data. The dataset used in this work can be downloaded from http://www.pnas.org/content/112/20/6389/tab-figures-data. The dataset consists on interpolated time series of the rocky intertidal community, the monthly sea temperature, monthly wind speed and monthly wave height. The community is composed by three species, namely: the honeycomb barnacle *Chamaesipho columna*, crustose brown alga *Ralfsia cf confusa* and little black mussel *Xenostrobus pulex*. The species interact on bare rock. The time series of species abundance has 250 data points sampled monthly from 1987–2008. A detailed analysis of the time series can be found in the original paper[25]. Following the reference, all species contributed to the dynamics (this is also illustrated in Supplementary Fig. 8 where we show that all species are included in the causal network).

Causal analysis. To determine whether the correlations between environmental variables and structural stability are spurious or reflect a causal relation, we performed a nonlinear causality test known as CCM[6]. CCM is an extension of standard Granger causality. However, in contrast with Granger causality, it can be used to test for causation in nonlinear dynamical systems, and requires convergence to large forecasting skills as the number of points included in the test increases. Importantly, because CCM is based on Taken's theorem, the results of the CCM test depend strongly on the choice of the embedding dimension used to compute the pairwise causal links. Hence, we focused particular attention on choosing the correct embedding dimension by running numerous tests with different embedding dimensions (from 1–20) and picking the one that maximizes the cross-mapping skills. To ensure causality, we need to show convergence and significance against a randomized version of the time-series data. To test for the statistical significance of the results, we ran the test with an ensemble of randomized versions of the time series, and plotted the results from the true time series against the 95th percentile of the random analysis. This provided a 95% significance level on the causal links. Surrogate time series were generated using the surrogate package in R. Using standard approaches[33,34], we generated surrogate data so that the original and randomized time series had the same power spectrum (that is, the Fourier transform of the original data and the surrogate ensemble only differed in their phase, which was randomized, but the amplitude was preserved). CCM skills (measured as correlation coefficients, ρ) were considered significant if they were above the random expectations. In addition, we computed the significance of the observed causal links against different null models. This was performed using the make_surrogate_data() function in the R package rEDM with method=seasonal and T_period=12. We found that the statistical significance of the causal link between sea temperature and structural stability was preserved under a null model that took into account possible seasonal bias (see Supplementary Fig. 10). All of the other links showed stronger statistical significance against the seasonal null model.

Reporting Summary. Further information on research design is available in the Nature Research Reporting Summary linked to this article.

Data availability

The data used in the manuscript can be downloaded from Benincà et al.[25] (http://www.pnas.org/content/112/20/6389/tab-figures-data).

Code availability

The code accompanying the manuscript is available on GitHub at https://github.com/MITEcology/Nature.Eco.Evo-Cenci-Saavedra-2019.git. The repository contains the code used to generate Figs. 3–5 and an illustrative example of how to compute the VCR from a multivariate time series.

Received: 13 August 2018; Accepted: 20 March 2019;
Published online: 29 April 2019

References

1. Levins, R. *Evolution in Changing Environments: Some Theoretical Explorations (Monographs in Population Biology)* (Princeton Univ. Press, 1968).
2. Thomas, C. D. et al. Extinction risk from climate change. *Nature* **427**, 145–148 (2004).
3. Chase, E. & Harwood, V. J. Comparison of the effects of environmental parameters on growth rates of *Vibrio vulnificus* biotypes I, II, and III by culture and quantitative PCR analysis. *Appl. Environ. Microbiol.* **77**, 4200–4207 (2011).
4. Montoya, J. & Raffaelli, D. Climate change, biotic interactions and ecosystem services. *Phil. Trans. R. Soc. B* **365**, 2013–2018 (2010).

5. Thackeray, S. J. et al. Phenological sensitivity to climate across taxa and trophic levels. *Nature* **535**, 241–245 (2016).
6. Sugihara, G. et al. Detecting causality in complex ecosystems. *Science* **338**, 496–500 (2012).
7. Dai, L., Vorselen, D., Korolev, K. S. & Gore, J. Generic indicators for loss of resilience before a tipping point leading to population collapse. *Science* **336**, 1175–1177 (2012).
8. Andronov, A. & Pontrjagin, L. Systémes grossiers. *Dokl. Akad. Nauk SSSR* **14**, 247–251 (1937).
9. Smale, S. Differentiable dynamical systems. *Bull. Am. Math. Soc.* **73**, 747–817 (1967).
10. Thom, R. *Structural Stability and Morphogenesis* (Addison-Wesley, 1994).
11. Allen, P. M. Evolution, population dynamics, and stability. *Proc. Natl Acad. Sci. USA* **73**, 665–668 (1976).
12. Rohr, R. P., Saavedra, S. & Bascompte, J. On the structural stability of mutualistic systems. *Science* **345**, 1253497 (2014).
13. Arnoldi, J.-F. & Haegeman, B. Unifying dynamical and structural stability of equilibria. *Proc. R. Soc. Lond. A* **472**, 20150874 (2016).
14. Cenci, S. & Saavedra, S. Structural stability of nonlinear population dynamics. *Phys. Rev. E* **97**, 012401 (2018).
15. Song, C., Rohr, R. P. & Saavedra, S. A guideline to study the feasibility domain of multi-trophic and changing ecological communities. *J. Theor. Biol.* **450**, 30–36 (2018).
16. Wood, S. N. & Thomas, M. B. Super–sensitivity to structure in biological models. *Proc. R. Soc. Lond. B* **266**, 565–570 (1999).
17. Perretti, C. T., Munch, S. B. & Sugihara, G. Model free forecasting outperforms the correct mechanistic model for simulated and experimental data. *Proc. Natl Acad. Sci. USA* **110**, 5253–5257 (2013).
18. Ye, H. et al. Equation-free mechanistic ecosystem forecasting using empirical dynamic modeling. *Proc. Natl Acad. Sci. USA* **112**, E1569–E1576 (2015).
19. Benincà, E. et al. Chaos in a long-term experiment with a plankton community. *Nature* **451**, 822–825 (2008).
20. Bjørnstad, O. N. & Grenfell, B. T. Noisy clockwork: time series analysis of population fluctuations in animals. *Science* **293**, 638–643 (2001).
21. Ushio, M. et al. Fluctuating interaction network and time-varying stability of a natural fish community. *Nature* **554**, 360–363 (2018).
22. Costantino, R. F., Desharnais, R. A., Cushing, J. M. & Dennis, B. Chaotic dynamics in an insect population. *Science* **275**, 389–391 (1997).
23. Turchin, P. & P. Ellner, S. Living on the edge of chaos: population dynamics of fennoscandian voles. *Ecology* **81**, 3099–3116 (2000).
24. Becks, L., Hilker, F. M., Malchow, H., Jürgens, K. & Arndt, H. Experimental demonstration of chaos in a microbial food web. *Nature* **435**, 1226–1229 (2005).
25. Benincà, E., Ballantine, B., Ellner, S. P. & Huisman, J. Species fluctuations sustained by a cyclic succession at the edge of chaos. *Proc. Natl Acad. Sci. USA* **112**, 6389–6394 (2015).
26. Deyle, E, R., May, R. M., Munch, S. B. & Sugihara, G. Tracking and forecasting ecosystem interactions in real time. *Proc. R. Soc. Lond. B* **283**, 20152258 (2016).
27. Sugihara, G. Nonlinear forecasting for the classification of natural time series. *Phil. Trans. R. Soc. Lond. A* **348**, 477–495 (1994).
28. Cenci, S., Sugihara, G. & Saavedra, S. Regularized S-map for inference and forecasting with noisy ecological time series. *Methods Ecol. Evol.* https://doi.org/10.1111/2041-210X.13150 (2019).
29. Cenci, S. & Saavedra, S. Uncertainty quantification of the effects of biotic interactions on community dynamics from nonlinear time-series data. *J. R. Soc. Interface* **15**, 20180695 (2018).
30. Helmuth, B. S. T. & Hofmann, G. E. Microhabitats, thermal heterogeneity, and patterns of physiological stress in the rocky intertidal zone. *Biol. Bull.* **201**, 374–384 (2001).
31. Harley, C. D. G. & Helmuth, B. S. T. Local and regional scale effects of wave exposure, thermal stress, and absolute versus effective shore level on patterns of intertidal zonation. *Limnol. Oceanogr.* **48**, 1498–1508 (2003).
32. Hastie, T., Tibshirani, R. & Friedman, J. *The Elements of Statistical Learning: Data Mining, Inference, and Prediction* (Springer, 2001).
33. Kantz, H. & Schreiber, T. *Nonlinear Time Series Analysis* (Cambridge Univ. Press, 2004).
34. Theiler, J., Eubank, S., Longtin, A., Galdrikian, B. & Farmer, J. D. Testing for nonlinearity in time series: the method of surrogate data. *Physica D* **58**, 77–94 (1992).
35. Mees, A. *Nonlinear Dynamics and Statistics* (Birkhäuser, 2011).
36. Mayo-Wilson, C. Structural chaos. *Phil. Sci.* **82**, 1236–1247 (2015).
37. Strogatz, S. *Nonlinear Dynamics and Chaos. With Applications to Physics, Biology, Chemistry, and Engineering (Studies in Nonlinearity)* (CRC Press, 2014).
38. Saavedra, S. et al. A structural approach for understanding multispecies coexistence. *Ecol. Monogr.* **87**, 470–486 (2017).
39. Nese, J. M. Quantifying local predictability in phase space. *Physica D* **35**, 237–250 (1989).
40. Song, C. & Saavedra, S. Structural stability as a consistent predictor of phenological events. *Proc. R. Soc. B* **285**, 20180767 (2018).

Acknowledgements

We thank C. Song for insightful discussions. Funding was provided by MIT Research Committee funds and the Mitsui Chair (S.S.).

Author contributions

S.C. and S.S. designed the study. S.C. performed the study. S.S. supervised the study. S.C. and S.S. wrote the paper.

Competing interests

The authors declare no competing interests.

Additional information

Supplementary information is available for this paper at https://doi.org/10.1038/s41559-019-0879-1.

Reprints and permissions information is available at www.nature.com/reprints.

Correspondence and requests for materials should be addressed to S.C.

Publisher's note: Springer Nature remains neutral with regard to jurisdictional claims in published maps and institutional affiliations.

nature research

Corresponding author(s): Simone Cenci

Last updated by author(s): 25/02/2019

Reporting Summary

Nature Research wishes to improve the reproducibility of the work that we publish. This form provides structure for consistency and transparency in reporting. For further information on Nature Research policies, see Authors & Referees and the Editorial Policy Checklist.

Statistics

For all statistical analyses, confirm that the following items are present in the figure legend, table legend, main text, or Methods section.

n/a	Confirmed	
☐	☒	The exact sample size (*n*) for each experimental group/condition, given as a discrete number and unit of measurement
☐	☒	A statement on whether measurements were taken from distinct samples or whether the same sample was measured repeatedly
☐	☒	The statistical test(s) used AND whether they are one- or two-sided *Only common tests should be described solely by name; describe more complex techniques in the Methods section.*
☐	☒	A description of all covariates tested
☐	☒	A description of any assumptions or corrections, such as tests of normality and adjustment for multiple comparisons
☐	☒	A full description of the statistical parameters including central tendency (e.g. means) or other basic estimates (e.g. regression coefficient) AND variation (e.g. standard deviation) or associated estimates of uncertainty (e.g. confidence intervals)
☐	☒	For null hypothesis testing, the test statistic (e.g. *F*, *t*, *r*) with confidence intervals, effect sizes, degrees of freedom and *P* value noted *Give P values as exact values whenever suitable.*
☒	☐	For Bayesian analysis, information on the choice of priors and Markov chain Monte Carlo settings
☒	☐	For hierarchical and complex designs, identification of the appropriate level for tests and full reporting of outcomes
☒	☐	Estimates of effect sizes (e.g. Cohen's *d*, Pearson's *r*), indicating how they were calculated

Our web collection on statistics for biologists contains articles on many of the points above.

Software and code

Policy information about availability of computer code

Data collection	*Provide a description of all commercial, open source and custom code used to collect the data in this study, specifying the version used OR state that no software was used.*
Data analysis	The data were analyzed using custom algorithms that we made freely available on GitHub (the link is provided in the main text)

For manuscripts utilizing custom algorithms or software that are central to the research but not yet described in published literature, software must be made available to editors/reviewers. We strongly encourage code deposition in a community repository (e.g. GitHub). See the Nature Research guidelines for submitting code & software for further information.

Data

Policy information about availability of data

All manuscripts must include a data availability statement. This statement should provide the following information, where applicable:

- Accession codes, unique identifiers, or web links for publicly available datasets
- A list of figures that have associated raw data
- A description of any restrictions on data availability

The dataset used in this work can be downloaded from http://www.pnas.org/content/112/20/6389/tab-figures-data

Field-specific reporting

Please select the one below that is the best fit for your research. If you are not sure, read the appropriate sections before making your selection.

☐ Life sciences ☐ Behavioural & social sciences ☒ Ecological, evolutionary & environmental sciences

Ecological, evolutionary & environmental sciences study design

All studies must disclose on these points even when the disclosure is negative.

Study description	A nonparametric framework is presented for estimating the local structural stability of ecological communities under environmental changes, including an application to empirical data.
Research sample	We analyzed both synthetic and empirical datasets. Synthetic data were generated with numerical integration of the differential equations provided in the Supplementary Information Empirical data were downloaded from http://www.pnas.org/content/112/20/6389/tab-figures-data The dataset consists on interpolated time series of the rocky intertidal community, the monthly sea temperature, monthly wind speed, and monthly wave height. The community is composed by three species, namely: the honeycomb barnacle (Chamaesipho columna), the (crustose) brown alga (Ralfsia cf confusa) , and the little black mussel (Xenostrobus pulex). The species interact on bare rock. The time series of species abundance has 250 data points sampled monthly from 1987 to 2008.
Sampling strategy	*Note the sampling procedure. Describe the statistical methods that were used to predetermine sample size OR if no sample-size calculation was performed, describe how sample sizes were chosen and provide a rationale for why these sample sizes are sufficient.*
Data collection	*Describe the data collection procedure, including who recorded the data and how.*
Timing and spatial scale	*Indicate the start and stop dates of data collection, noting the frequency and periodicity of sampling and providing a rationale for these choices. If there is a gap between collection periods, state the dates for each sample cohort. Specify the spatial scale from which the data are taken*
Data exclusions	*If no data were excluded from the analyses, state so OR if data were excluded, describe the exclusions and the rationale behind them, indicating whether exclusion criteria were pre-established.*
Reproducibility	The Figures can be reproduced using the code that we deposited on GitHub available at the link provided in the main text.
Randomization	*Describe how samples/organisms/participants were allocated into groups. If allocation was not random, describe how covariates were controlled. If this is not relevant to your study, explain why.*
Blinding	*Describe the extent of blinding used during data acquisition and analysis. If blinding was not possible, describe why OR explain why blinding was not relevant to your study.*

Did the study involve field work? ☐ Yes ☒ No

Reporting for specific materials, systems and methods

We require information from authors about some types of materials, experimental systems and methods used in many studies. Here, indicate whether each material, system or method listed is relevant to your study. If you are not sure if a list item applies to your research, read the appropriate section before selecting a response.

Materials & experimental systems

n/a	Involved in the study
☒	☐ Antibodies
☒	☐ Eukaryotic cell lines
☒	☐ Palaeontology
☒	☐ Animals and other organisms
☒	☐ Human research participants
☒	☐ Clinical data

Methods

n/a	Involved in the study
☒	☐ ChIP-seq
☒	☐ Flow cytometry
☒	☐ MRI-based neuroimaging